



Interferometric Method for Monitoring Electrochemical Etching of Thin Films

Z. Gaburro,^z C. J. Oton, P. Bettotti, L. Dal Negro, G. Vijaya Prakash, M. Cazzanelli, and L. Pavesi

INFM and Dipartimento di Fisica, Università degli Studi di Trento, Italy

In this work we present a method for monitoring the optical parameters of a film during its etching process. Optical interferometry of two laser beams with different angles of incidence is observed to measure the index of refraction profile and the etch rate evolution simultaneously. With this technique we have measured the inhomogeneity in the etch process of porous silicon layers, which is an essential issue to make good quality optical microcavities or photonic crystals with this material. In addition, by sweeping a range of currents we are able to fully characterize the etch rate and the porosity vs. current density in one single sample, without the need of independent measurements.

© 2003 The Electrochemical Society. [DOI: 10.1149/1.1568110] All rights reserved.

Manuscript submitted November 8, 2001; revised manuscript received December 13, 2002. Available electronically April 10, 2003.

In recent years, much attention has been paid to the formation of porous silicon layers by electrochemical etching due to their easy, low-cost process.¹⁻⁶ Optical devices such as distributed Bragg reflectors (DBRs), optical resonators, or filters are among the most promising applications of these porous silicon layers.⁸⁻¹¹ In order to make high-quality optical devices, we need a very accurate knowledge of the etch rate and porosity. These parameters have been characterized under different growth conditions.^{2,5,7} At fixed current density, concentration of the electrolyte, and temperature, a constant etch rate is usually assumed, as well as a homogeneous index of refraction of the layer. Although approximate, this assumption is reasonable, as experimentally demonstrated, and convenient, due to the difficulty in measuring deviations from constant etch rates. However, it has been proved that this assumption is not exact by postgrowth characterization, such as photoluminescence (PL) and Raman spectroscopy measurements of freestanding layers,¹²⁻¹⁴ ellipsometry,¹⁵ and calorimetry.¹⁶ The magnitude of these deviations from constant etch rate and constant porosity is a critical issue for optical devices based on interference between stacked porous silicon layers.^{4,5}

Using *in situ* single-beam interference, Thönissen *et al.* have shown inhomogeneities in the optical thickness during the growth of the porous silicon layers.¹⁴ In general, the sign of the porosity gradient with depth depends on the resistivity of the silicon wafers employed and on the concentration of the electrolyte. For lightly doped silicon, the porosity decreases with depth, but for heavily doped p⁺ wafers an increase is observed.¹²⁻¹⁴ The *in situ* single-beam interference technique can also be applied to other thin-film growth processes, such as molecular beam epitaxy or chemical vapor deposition (CVD).^{18,19} Alius and Schmidt also described a two-beam method to find the value of the index of refraction and the depth of the CVD grown film by making use of two interference patterns of laser beams with different angles of incidence.¹⁷ However, with the approach we present, the refractive index profile of the layer can be monitored as well as the etch rate variations with time.

Theory

In order to analyze the interference signal observed at the output, the ray equation has to be solved inside the inhomogeneous layer. We assume that the index of refraction is only dependent on the depth variable x and not on the other coordinates y, z ; hence, lateral inhomogeneities are not taken into account.⁴ To solve the problem we divide the porous layer into an infinite number of layers of differential depths and continuous variation of indexes of refraction. Within this approach, the ray gets refracted as it passes through

every differential depth with a deviation given by Snell's law. It can be shown that the optical path difference D between the beam reflected on the etched surface and the one reflected on the bulk is

$$D = 2 \int_0^l \sqrt{n(x)^2 - n_{\text{HF}}^2 \sin^2 \theta} dx + \varphi_0 - \varphi_1 \quad [1]$$

where l is the depth of the layer, $n(x)$ is its index profile, n_{HF} is the index of refraction of the electrolyte, θ is the angle of incidence of the beam when it arrives to the etched surface, and φ_0 and φ_1 are the phase changes produced in the reflection of each beam on the upper interface and on the buried one. In our case, l is a function of time, and we approximate the quantities φ_0 and φ_1 as constants. The quantity we measure experimentally is not the optical path difference but its change rate dD/dt . The oscillations in the output signal have a frequency which is proportional to this change rate as

$$\nu(t) = \frac{1}{\lambda_0} \frac{dD}{dt} \quad [2]$$

where λ_0 is the vacuum wavelength of the beam. The rate of change of D can be in general calculated using the Leibnitz formula

$$D(t) = \int_{a(t)}^{b(t)} f(t, \xi) d\xi$$
$$\frac{dD}{dt} = \left[f(t, b(t)) \frac{db}{dt} \right] - \left[f(t, a(t)) \frac{da}{dt} \right] + \left[\int_{a(t)}^{b(t)} \frac{\partial f(t, \xi)}{\partial t} d\xi \right] \quad [3]$$

We assume that $n(x)$, for any given x , does not depend on time. This is equivalent to saying that during the electrochemical etching, no other effect changes the value of the refractive index at a given x . For instance, we neglect any chemical etching that is simultaneous to the electrochemical one. Validity of this assumption is supported by the results obtained here and is consistent with other works,¹³ considering the low concentration of the electrolyte employed. Thus, within this approximation, we obtain

$$\nu(t) = \frac{1}{\lambda_0} 2 \sqrt{n^2(l) - n_{\text{HF}}^2 \sin^2 \theta} \frac{dl}{dt} \quad [4]$$

which is the frequency of the oscillations observed with an incident angle θ .

Finally, by algebraic manipulations and given the frequencies ν_1 and ν_2 for two different angles θ_1 and θ_2 , we can solve the equation for the index profile and the etch rate

^z E-mail: gaburro@science.unitn.it

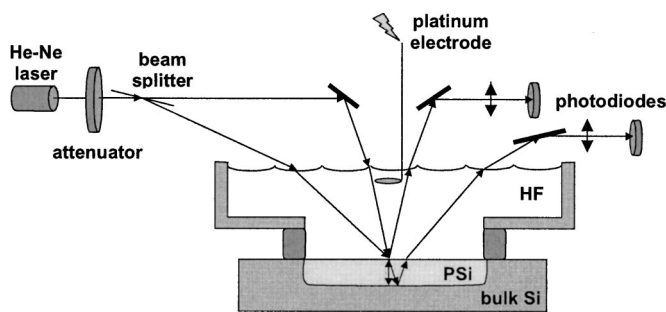


Figure 1. Setup of the experiment. The angles of incidence of each beam onto the sample were 8 and 38°.

$$\begin{cases} n(t) = n_{\text{HF}} \sqrt{\frac{v_1^2(t) \sin^2 \theta_2 - v_2^2(t) \sin^2 \theta_1}{v_1^2(t) - v_2^2(t)}} \\ \frac{dl(t)}{dt} = \frac{\lambda_0}{2n_{\text{HF}}} \sqrt{\frac{v_1^2(t) - v_2^2(t)}{\sin^2 \theta_2 - \sin^2 \theta_1}} \end{cases} \quad [5]$$

We have employed these equations for the estimation of the growth parameters.

The use of two beams instead of one allows a clear separation of physical thickness from the index of refraction. In fact, the oscillations of reflectivity are originated by the time evolution of differences between optical paths, where thickness and index of refraction are mixed together as in Eq. 4.

Experimental

The porous silicon samples were fabricated using boron-doped p^+ silicon substrates of low resistivity (0.01 Ω cm). A 13% HF electrolyte was employed, prepared by dilution of standard 48 wt % aqueous HF with ethanol. The area of silicon exposed to the electrolyte is shown in Fig. 1. The light source was a He-Ne 5 mW polarized laser beam and was attenuated down to 300 nW. This low power level assures no effect of the light beam on the anodization.¹⁴ We split the laser light to have one beam at quasi-normal incidence (8°) and the other at an angle of 38°, impinging on the sample in the same spot. The two reflected signals were collected into two silicon photodiodes by means of lenses. The current signal of each photodiode was amplified and acquired by a personal computer, which simultaneously controlled the current source of the chemical etch (a Keithley 2400). The anodization was performed in the dark.

Figure 2 shows the oscillating intensity of both reflected beams, obtained using a constant etching current (current density 25 mA/cm²). The oscillations of the two signals have clearly different frequencies due to the different angles of the beams. The sporadic spikes on the signal are due to the gas bubbles which came out from the sample and from the platinum electrode. In this technique, the etching current density does not need to be constant in time.

Discussion

We have first characterized the variation of the etch rate and porosity with time for a constant current. This is the easiest experimental framework to test the measurability of the frequency of oscillations, the key quantity for Eq. 5. The current density selected for this was 25 mA/cm² in order to have an intermediate porosity ($\approx 58\%$).

The two different frequencies of the oscillating signals on Fig. 2, corresponding to the two different angles, have been extracted from the position of every maximum. This gave us two scattered plots of frequencies at discrete times. An adjacent-average smooth interpolation was used to plot continuously the index of refraction and the etch rate vs. time. The index of refraction has been used to estimate the porosity (volumetric fraction of silicon dissolved) by making use

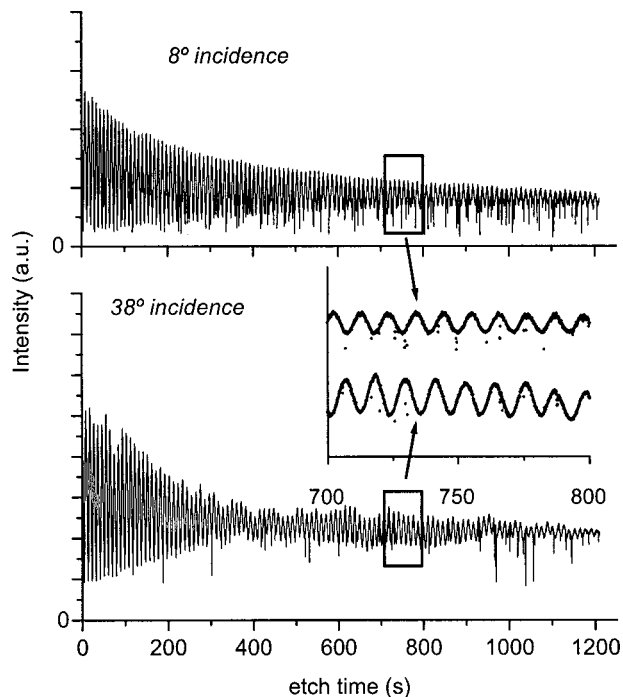


Figure 2. Intensity of reflected beams vs. time during anodization. The sporadic spikes are due to bubbles which deviated or scattered the laser beams.

of the Bruggeman effective-medium approximation.^{5,6} In the Bruggeman formula, we used $n = 3.8$ for silicon and $n = 1.35$ for the solution. Results are displayed in Fig. 3. A clearly observable

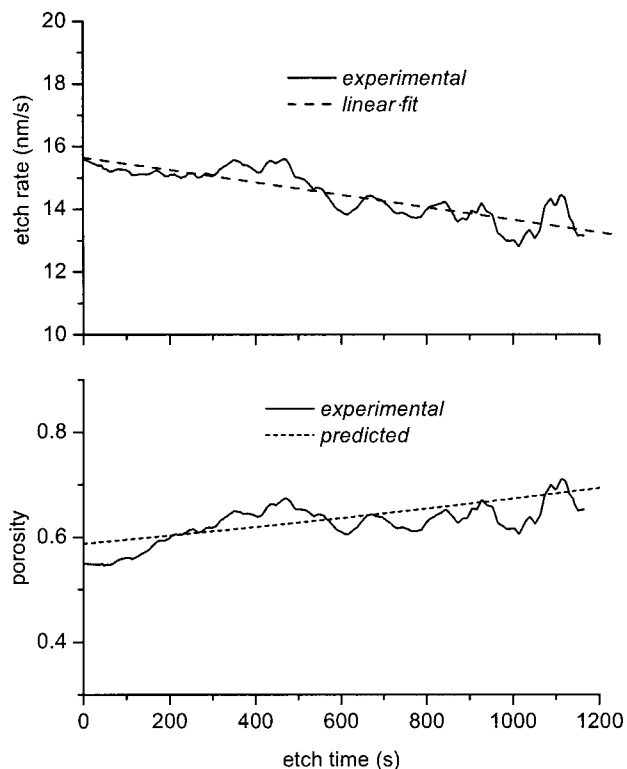


Figure 3. Etch rate and porosity evolution from data of Fig. 2. Top plot shows (—) etch rate vs. time and (---) its linear fit. Bottom plot shows porosity vs. time (—) directly extracted from experimental data and (····) from the linear fit of the etch rate and Eq. 6.

trend of data is a decrease of etch rate and an increase of porosity with etching time, *i.e.*, with depth. This coupled tendency is consistent with the simplest model of the etching progress, where the etch rate and the porosity are inversely proportional. This simple model is discussed as follows. The amount of silicon volume per unit area per unit time removed by the electrochemical etching is $(dl/dt)p$, where p is the porosity. The required charge to remove a unit volume of silicon is Nev , where N is the number of silicon atoms per volume unit ($5 \times 10^{22} \text{ cm}^{-3}$), e the electronic charge, and v the valence of the electrochemical reaction, *i.e.*, the number of electrons required for the removal of a single silicon atom. Thus

$$\frac{dl}{dt}p = \frac{j}{Nev} \quad [6]$$

where j is the current density. If a constant valence of the electrochemical process is assumed and a constant current density is forced, the etch rate and the porosity are inversely proportional.

According to this simple model, the profile of porosity with depth can be predicted from the profile of etch rate. Assuming a constant valence of 3.4 according to previous works^{20,21} and plugging the smoothly fitted etch rate (Fig. 3, top plot) into Eq. 6, we have obtained the predicted porosity shown in Fig. 3, bottom plot. This porosity can be compared with the porosity calculated via the Bruggeman formula from the measured index of refraction. As seen, considering the simplicity of the model, the agreement is very good. The increase of porosity with depth also agrees with other works^{12,14} which conclude that in p^+ -type porous silicon the nanocrystal size decreases with depth.

We have checked the accuracy of this method by independently measuring the depths of some layers using cross-sectional scanning electron microscopy (SEM) micrographs. Comparing these depths with the integration of the etch rate curve we have found total agreement within an error of less than 5%.

Once the degree of accuracy has been tested, we have considered other situations beyond the simple constant etching current operation. Several features of the electrochemical etching of porous silicon might be quantitatively measured with this technique. For example, the effect of etch stops, *i.e.*, regular interruptions in time of the etching current to allow solution exchange can be characterized. It has been shown that etch stops can have a beneficial impact on regularity and homogeneity of the porous silicon structure.¹³ We have calculated the etch rate just after a current stop of 2 min after the 20 min etch shown in Fig. 2. We found a value of 14.9 nm/s after the etch stop, whereas the value just before the stop was 13.3 nm/s. It can be concluded that the etch stop of 2 min has made possible a regeneration of the HF concentration which restores the growth conditions to values similar to the beginning.¹³

Another appealing peculiarity of the proposed technique is the possibility of running a complete characterization of etch rate and porosity *vs.* etching current density using a single sample for a given solution and a given substrate doping. Our theoretical approach applies to a general case, where the etch rate and index of refraction can change arbitrarily. Therefore, the theory is not limited to the case of constant current density but is also valid for time-varying currents. In practice, the variations must be slow enough to allow reliable frequency estimation. If the etching current is swept in time between two suitable values, we can extract the complete etching rate table, as well as the respective refractive index, for the whole range of current densities applied. To illustrate the technique with a variable current sweep, we have first chosen a total duration of 400 s. This duration was suggested by the results of Fig. 3, which shows that depth inhomogeneities are negligible in such a time interval. The measurement is best performed if a longer time is dedicated to lower current density values, since they imply slower signal oscillations. Figure 4 shows the sweep of etching current density from 5 to 80 mA/cm^2 (right axis) and the periods of the oscillation in the intensity of the reflected beam (left axis). From data of Fig. 4, the etch rate and porosity profiles *vs.* current density could be obtained,

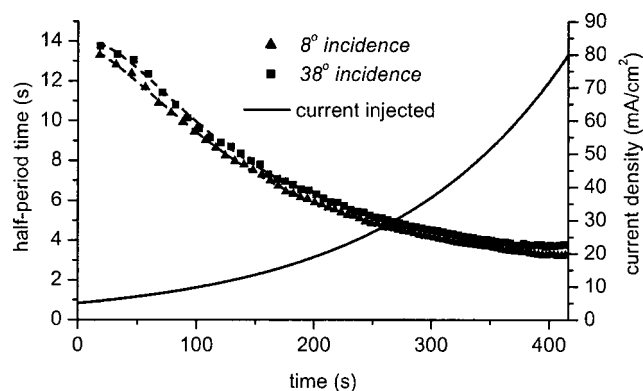


Figure 4. Anodization performed with time-varying current density. The sweep was performed from 5 to 80 mA/cm^2 (right axis). On the left axis, the graph reports the time interval between two consecutive zero-derivative points in the reflected beam intensity. This interval corresponds to a half period of the oscillating intensity.

as reported in Fig. 5. Both the etch rate and the porosity increase with the etching current density. Porous silicon etch rates are usually fitted to a power function as⁷

$$\frac{dl}{dt} = Aj^k \quad [7]$$

where A is an arbitrary constant, j is the current density, and k is a constant, which is usually ≈ 0.8 , regardless of the resistivity and the HF concentration.⁷ We have fitted our curve to the same function and see good agreement using $k = 0.7$, which is close to the expected one. Finally, the porosity dependence can be fitted to a line. If we compare our result with the porosities measured with other techniques^{5,6} we can also find good agreement. We stress here that

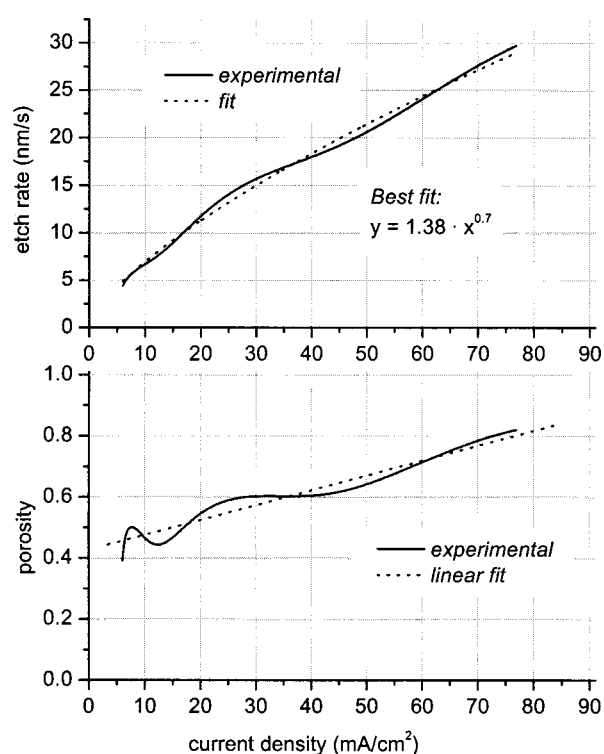


Figure 5. Etch rate and porosity curves *vs.* current density measured on sample of Fig. 4.

this technique requires a single sample and no other experimental technique (such as, for example, SEM). Both features are important strategic factors when the porous layer must be optimized for the applications, since the waste of time, silicon substrates, and hydrofluoric acid is reduced to a minimum.

Conclusions

In the present work we have described a simple and innovative technique for the characterization of etch rate and porosity during the growth of an electrochemical etched layer of p⁺-doped silicon. A good estimation of these parameters and their dependence with time is very valuable information for the fabrication of good-quality optical multilayers. We have shown that this technique gives us values in accordance with other experimental methods. We have found that after 20 min of etching, the growth rate diminishes by 15%. Accordingly, we observed an increase of porosity, which agrees with a constant-valence approximation. Finally, we have shown that by sweeping the etching current density with time, a complete characterization of the etch parameters can be performed using a single sample, thus minimizing the waste of time, silicon, and hydrofluoric acid.

Acknowledgments

This work has been supported by the INFM progetto PAIS-SMOG.

Università degli Studi di Trento assisted in meeting the publication costs of this article.

References

1. L. T. Canham, *Appl. Phys. Lett.*, **57**, 1046 (1990).
2. M. I. J. Beale, J. D. Benjamin, M. J. Uren, N. G. Chew, and A. G. Cullis, *J. Cryst. Growth*, **73**, 622 (1985).
3. P. M. Fauchet, *J. Lumin.*, **70**, 294 (1996).
4. A. G. Cullis, L. T. Canham, and P. D. J. Calcott, *J. Appl. Phys.*, **82**, 909 (1997).
5. L. Pavesi, *Riv. Nuovo Cimento*, **20(10)**, 1 (1997).
6. W. Theiß, *Surf. Sci. Rep.*, **29(3/4)**, 91 (1997).
7. E. Haimi, V. K. Lindroos, and R. Nowak, *J. Nanosci. Nanotech.*, **1(2)**, 201 (2001).
8. M. G. Berger, C. Dieker, M. Thönissen, L. Vescan, H. Lüth, H. Munder, W. Theiß, M. Wernke, and P. Grosse, *J. Phys. D*, **27**, 1333 (1994).
9. C. Mazzoleni and L. Pavesi, *Appl. Phys. Lett.*, **67**, 1983 (1995).
10. M. G. Berger, R. Arens-Fischer, M. Thönissen, M. Krüger, S. Billat, H. Lüth, S. Hilbrich, W. Theiß, and P. Grosse, *Thin Solid Films*, **297**, 237 (1997).
11. G. Lammel, S. Schweizer, and Ph. Renaud, *Sens. Actuators A*, **92**, 52 (2001).
12. M. Thönissen, S. Billat, M. Krüger, H. Lüth, M. G. Berger, U. Frotscher, and U. Rossow, *J. Appl. Phys.*, **80**, 2990 (1996).
13. S. Billat, M. Thönissen, R. Arens-Fischer, M. G. Berger, M. Krüger, and H. Lüth, *Thin Solid Films*, **297**, 22 (1997).
14. M. Thönissen, M. G. Berger, S. Billat, R. Arens-Fischer, M. Krüger, H. Lüth, W. Theiß, S. Hilbrich, P. Grosse, G. Lerondel, and U. Frotscher, *Thin Solid Films*, **297**, 92 (1997).
15. C. Pickering, L. T. Canham, and D. Brumhead, *Appl. Surf. Sci.*, **63**, 22 (1993).
16. C. Faivre, D. Bellet, and G. Dolino, *Eur. Phys. J. B*, **7**, 19 (1999).
17. H. Alius and R. Schmidt, *Rev. Sci. Instrum.*, **61**, 1200 (1990).
18. Ching-Hsong Wu, W. H. Weber, T. J. Potter, and M. A. Tamor, *J. Appl. Phys.*, **73**, 2977 (1993).
19. Y. He, B. W. Sheldon, and T. F. Morse, *IEICE Trans. Electron.*, **E83-C(3)**, 315 (2000).
20. Z. Gaburro, H. You, and D. Babić, *J. Appl. Phys.*, **84**, 6345 (1998).
21. X. G. Zhang, *J. Electrochem. Soc.*, **138**, 3750 (1991).